steady-state source of background which could possibly offset the gain in flux by reducing the accuracy of the intensity measurements. In the case of NiF_2, an LT data set was collected under each of the two conditions. From Table 2, it is obvious that the results are hardly affected and certainly not contaminated by the increase in the delayed neutron background.

We wish to thank Dr I. R. Jahn for the loan of the samples. The work at Argonne was supported by the Office of Basic Energy Sciences Division of Materials Sciences, US Department of Energy, under contract W-31-109-Eng-38.

References

BECKER, P. J. & COPPENS, P. (1974). *Acta Cryst.* A**30**, 129–147.
EPPERSON, J. E., CARPENTER, J. M., THIYAGARAJAN, P. & HEUSER, B. (1990). *Nucl. Instrum. Methods*, A**289**, 30–34.
HAEFNER, K. (1964). Thesis, Univ. of Chicago, USA.
HAEFNER, K., STOUT, J. W. & BARRETT, C. S. (1966). *J. Appl. Phys.* **37**, 449–450.
JAHN, I. R. (1973). *Phys. Status Solidi B*, **57**, 681–692.
JAUCH, W. (1991). *Phys. Rev. B*, **44**, 6864–6869.
JAUCH, W., MCINTYRE, G. J. & SCHULTZ, A. J. (1990). *Acta Cryst.* B**46**, 739–742.
JAUCH, W., SCHULTZ, A. J. & SCHNEIDER, J. R. (1988). *J. Appl. Cryst.* **21**, 975–979.
JAUCH, W. & STEWART, R. F. (1991). *Sagamore X Conference on Spin, Charge and Momentum Densities, Konstanz, Germany.* Abstracts, p. 58.
PALMER, A. & JAUCH, W. (1991). *Solid State Commun.* **77**, 95–97.
PALMER, A. & JAUCH, W. (1993). *Phys. Rev. B*, **46**. In the press.
SEARS, V. F. (1992). *International Tables for Crystallography*, Vol. C. Dordrecht: Kluwer.
WILKINSON, C. (1986). *J. Phys. (Paris) Colloq.* C5, **47**, 35–42.
ZACHARIASEN, W. H. (1967). *Acta Cryst.* **23**, 558–564.

Acta Cryst. (1993). B**49**, 987–996

Multistage Diffusionless Pathways for Reconstructive Phase Transitions: Application to Binary Compounds and Calcium Carbonate

BY ANDREW G. CHRISTY

Department of Chemistry, University of Leicester, Leicester LE1 7RH, England

(*Received* 26 *May* 1993; *accepted* 3 *August* 1993)

Abstract

The distinction between 'displacive' and 'reconstructive' phase transformations is subjective, but rigorous classification into three types is possible using symmetry criteria. Type I shows a group–subgroup relationship between phase symmetries corresponding to a unique irreducible representation of the higher symmetry. Type II transitions are those in which continuous change of a structural parameter relates stable phases through a shared subgroup or supergroup intermediate. Any other transition (type III) can be effected through a chain of type I or II steps. There is experimental evidence that some 'reconstructive' transitions use transformation paths involving only a small number (3–4) of steps, without descent in symmetry to an amorphous intermediate. Such short pathways may be particularly important at high pressure. However, longer routes and less symmetrical transition states may be favoured kinetically. The shortest pathways between structures are readily derived by considering structural similarities and available lattice modes. The probable utilization of such routes provides a rationale for understanding observed stable and metastable behaviour, as shown by examples from MX and MX_2 systems and $CaCO_3$. The predictions of this approach are readily tested using molecular dynamics simulations.

1. Introduction

Buerger (1951) classified structural phase transitions as *reconstructive* or *displacive*, depending on whether or not breakage of primary interatomic bonds was required in order to interconvert the crystal structures. There is a correlation with transformation mechanism in that reconstructive transitions are likely to involve heterogeneous nucleation, whereas new phases may nucleate homogeneously in a displacive transition. Thermodynamically, reconstructive transitions show discontinuities in first-order free-energy derivatives (entropy and volume) due to the significant change in atomic environments at the transition, whereas displacive transitions may be second-order in character. Even when a displacive transition is thermodynamically first order, the close relationship between the structures of the two phases makes it easy to visualize transformation occurring continuously, by variation of a few structural parameters. The first-order character then arises because these intermediate states are higher in energy at the transition than the structures of either stable phase.

The distinction between transformation types is by no means unambiguous. The presence or absence of a bond is only clearly defined in the case of directed, covalent bonding. Large structural distortions and coordination changes are found in martensitic and related transformations, despite the fact that transformation is diffusionless and continuous. Some workers classify these transformations as 'displacive' (Delaey, 1991) whereas others prefer to regard them as reconstructive (Dmitriev, Rochal, Gufan & Tolédano, 1988). The distinction is in fact gradational rather than dichotomous (Putnis & McConnell, 1979).

It is possible to define transformation types more rigorously using symmetry criteria. In this paper, transitions are divided into:

(i) Those showing an immediate group–subgroup symmetry relationship, that can be modelled thermodynamically using the Landau formalism.

(ii) Those where change in one set of structural parameters transforms the structure through an intermediate whose symmetry is a common subgroup or supergroup of the stable phases. Such transitions are modelled in the modified Landau theory of Dmitriev *et al.* (1988).

(iii) Those where the structures can be interconverted through a chain of distinct steps, each like (i) or (ii) above. Any transition not in classes (i) and (ii) falls into this category, as is argued below.

The three categories above will now be described in more detail.

2. Classes of phase transition

2.1. *Type* I *transitions*

For two structures related by very small atomic displacements, the space-group symmetries of the two phases are necessarily in a subgroup–supergroup relationship to one another since infinitesimal displacements may move atoms from a general site to a special site of the high-symmetry structure (thus causing a symmetry reduction) but not to another special site. Systems showing such behaviour have received much attention because the variation in physical properties of the phases across the transition may be related to structural variables using Landau theory (Landau & Lifshitz, 1958). Type I transitions are characterized by the following properties.

(i) The deviation of the structure of the low-symmetry (LS) phase from that of the high-symmetry (HS) phase may be described by an order parameter, η, which transforms as a non-identity, physically irreducible representation (IR) of the HS symmetry, and as the identity representation for LS.

(ii) The order parameter and powers of it are directly proportional to measurable strains and atomic coordinates to a close approximation.

(iii) The free-energy difference between HS and LS structures is represented as a polynomial in η with a small number of terms.

In practice, Landau theory is found to model LS thermodynamic properties surprisingly well for significant values of η. Furthermore, it provides stringent symmetry conditions that must be satisfied for a transition to be thermodynamically second order (Birman, 1966). Even when these conditions are met, negative coefficients for high-order terms in the free-energy polynomial may result in first-order thermodynamics. However, the predictions of the theory may not be accurate in the very small η régime near the transition point due to the occurrence of fluctuations. A recent review of applications and limitations is provided by Salje (1991).

2.2. *Type* II *transitions*

Recently, attempts have been made to model, using a Landau-like formalism, diffusionless transitions that do not satisfy conditions (i) and (ii) above (Dmitriev *et al.*, 1988). These workers note that the large atomic shifts and shears that occur in martensitic and similar phase transitions bring about a change in simple structures that is periodic with displacement. They quote the β and ω phases in Ti, Zr and Hf as an example.

The periodicity of the structural change is expressed by Dmitriev *et al.* (1988) in their definition of an order parameter, $\eta = a + b\sin(2\pi z + \varphi)$, where z is an atomic displacement and the other parameters are constants appropriate to the system being modelled. The free energy is then expressed as a Taylor expansion in η, as in the Landau approach. However, this corresponds to a Fourier series in $2\pi z$ since η and z are no longer linearly related.

The formalism of Dmitriev *et al.* (1988) predicts several potential stable phases corresponding to specific fixed values of η, each with a distinctive high symmetry. A free-energy minimum can also occur for one variable value of η, corresponding to the common LS phase. All HS phases may be regarded as special cases of the LS phase with constrained values of a specific set of structural variables. If each HS–LS transition were described in Landau theoretical terms, then the IRs of the various HS phases all correlate through the LS phase. Symmetrically, it would be valid to model an individual HS–LS step using Landau theory. In practice, the large displacements involved would make it difficult to reproduce the thermodynamics of the LS phase accurately.

For type I transitions, the HS–LS relationship is described by one IR of the HS phase. The lattice distortions and atomic displacements involved in the transition may therefore be correlated with softening of lattice vibrational modes of one particular symme-

try species. Martensitic transformations of the type described by Dmitriev *et al.* (1988) note that lattice mode softening is also implicated as a mechanism for the transitions that they consider, citing the experimental evidence of Ernst, Artner, Blaschko & Krexner (1986) on the b.c.c.–h.c.p. transition in lithium.

In summary, diffusionless transitions such as β–ω may occur by descent in symmetry from one stable structure (HS1) to a LS structure that is shared with the other stable phase (HS2). Specific lattice modes are utilized at each step, and are those consistent with considering the transition as a pair of back-to-back type I transitions. The modes do not need to soften to zero velocity since the intermediate LS phase has only a transitory existence as the intermediate state between HS phases.

Dmitriev, Rochal, Gufan & Tolédano (1989) describe transitions such as f.c.c.–h.c.p. where there is a common *higher* symmetry intermediate rather than one of *lower* symmetry. In this particular case, the ascent in symmetry corresponds to delocalization of atoms between sites that are distinguishable in the stable phase, and to stacking disorder. The intermediate for this interpolytypic transformation corresponds to the *superposition structure* of order–disorder theory (Dornberger-Schiff, 1959; Durovic & Weiss, 1986).

2.3. *Type* III *transitions*

Boyle, Walker & Wanjie (1980) suggested that symmetric correlations between the structures of phases should be looked for even where the obvious structural relationships of type I/II transitions are lacking, and that vibrational modes might play a rôle in determining atomic motions during transformations other than the classically 'displacive' ones. However, a general transformation between two specified structures requires more than one intermediate state.

It has already been seen that type II transitions can be regarded as two type I-like stages sharing a common LS or HS. In the former case, the LS symmetry must be compatible with single active IRs of both HS phases, the range of possible symmetries for {HS1, LS, HS2} is restricted for such a two-stage process. However, the possibilities increase if more stages are interpolated. The extra steps may be either:

(i) Further descent in symmetry. Site symmetries are reduced, and changes in lattice geometry and atomic coordinates may be achieved in accord with an IR of the LS phase, or:

(ii) Ascent in symmetry. Even if no additional degrees of structural freedom are gained by disordering atoms, the richer IR symmetry of the new HS phase allows descent into LS structures that would not otherwise be accessible.

It should be stressed that the IRs utilized do not have to be at the Brillouin zone centre. Successive descents in symmetry allow any structure to be reduced to $P1$ symmetry with an arbitrarily large unit cell, and then raised in symmetry to produce any other structure. Taken to the extreme, the symmetry reduction steps correspond to amorphization. Amorphous structures and the disordered structures associated with grain boundaries, line and plane defects, may therefore be regarded as the ultimate limit of descent in symmetry by a chain of HS–LS steps with atomic motions determined by permitted lattice vibrations at every step. Locally amorphous structures are important in all the transformation mechanisms associated with 'reconstructive' phase transitions, such as dissolution–reprecipitation, grain-boundary nucleation and propagation of defect arrays. Thus, the thermodynamic and symmetric treatments used for classically 'displacive' transitions can be extended to incorporate the reconstructive extreme as a special case. Even where transformation strains are too great for lattice coherence to be maintained during growth of a new phase, the initial nucleation step may be diffusionless, and nucleation kinetics modelled accordingly.

3. Multistage diffusionless transformation paths

Clearly, for transformation between any two structures, at least one shortest route exists. This may be found by comparing the structures of the stable phases for shared features, and finding lattice modes available in each phase that preserve these features while changing the rest of the structure. An infinitude of more complex paths can then be constructed by interpolating extra steps. These may be of interest since the route actually used will be the fastest rather than the shortest. That is, the route with the most stable highest-energy intermediate structure, and hence the lowest energy barrier. Under different conditions, it is possible that a relatively low-energy transition state would become a macroscopically observable phase, stable or metastable.

The utilization of short multistage transformation paths is suggested by two main lines of evidence.

(i) The observation of ephemeral transition states by diffraction or spectroscopy during transformation.

(ii) In many cases, analysis of the static and dynamic symmetry reveals that the predicted intermediates on short transformation paths between two stable phases occur macroscopically as metastable phases or as stable phases under other pressure–temperature conditions. Therefore, they are likely to

be relatively low in energy as transition states between more stable phases.

It was shown in Adams, Christy, Haines & Clark (1992) that there is evidence of both types for multi-stage diffusionless transformation in lead monoxide. The HS phases, litharge and massicot, are related by four interconnected three-step routes. The low-temperature (α') phase, . and the intermediate-pressure (γ) phase may both be generated from litharge by softening of the litharge E_u modes, which is also required to produce one of the litharge–massicot transition states. This transition state is involved in two of the three-step transformation routes. That the others are also used, and have a transient existence in domains large enough to diffract coherently, is suggested by additional peaks occurring in the X-ray data of Schoonover, Groy & Lin (1989).

It is particularly likely that short routes become kinetically important at high pressure. This is because the volume of activation for the transformation will tend to be larger for intermediate states that are very different from either stable structure than for intermediates that are more similar to the stable phases. Equivalently, it can be stated that pressure tends to inhibit 'free diffusion' of atoms.

The shortest possible paths and corresponding transition states between structures may be identified by inspection. Knowledge of them may be applied in a variety of ways.

(i) Understanding the symmetric relationships between phases can lead to very simple phenomenological modelling of whole phase diagrams [*cf.* Dmitriev, Gufan & Tolédano (1991) on α-, γ-, δ- and ε-Fe].

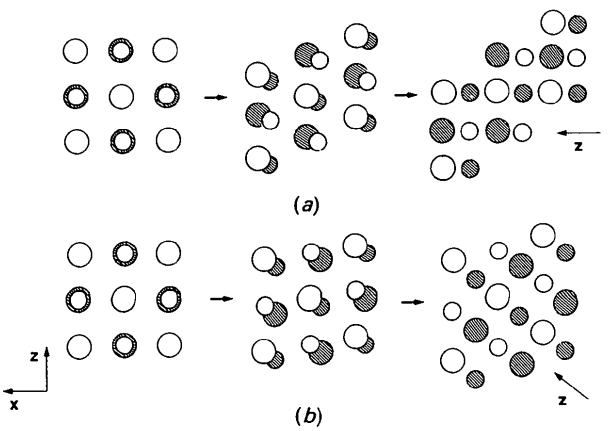

Fig. 1. (*a*) *B*1–*B*2 transformation *via* a *Cm* intermediate, using the zone-centre T_{1u} mode. Cations displaced relative to anions parallel to $[101]_{B1}$. (*b*) Transformation *via* a *Pnmm* intermediate, using the X_5^- zone-boundary mode. Top cation + anion layer shifted relative to lower one parallel to [101]. Large circles are cations, small ones are anions. Shading indicates height $(b/2)_{B1}$ below plane of paper.

(ii) Solid-state transformation mechanisms can be predicted and sought experimentally (*cf.* PbO).

(iii) Candidates for new stable structures (particularly at high pressure, where structural data may be limited) can be predicted.

(iv) Where it is known from experiment that long transformation paths are used ('reconstructive transformation'), it is equally implied that the transition states on shorter routes are very unstable. Since these states can be identified by consideration of the relationship between HS structures, the reasons for their instability can be investigated by lattice dynamic simulation.

The next section of this paper illustrates these applications, interpreting the transformation behaviour of simple binary compounds, and also the $CaCO_3$ phases, in terms of their shortest diffusionless tranformation paths.

4. Examples

4.1. *The B1–B2 transition*

Boyle *et al.* (1980) point out that it is impossible to transform from the *Fm*3*m* NaCl (*B*1) structure to *Pm*3*m* CsCl (*B*2) whilst maintaining both cubic symmetry and a $Z' = 1$ primitive unit cell. However, Shoji (1931) noted that both structures can be described using a rhombohedral cell with $\alpha = 60°$ for *B*1 and 90° for *B*2. No change in atomic coordinates is required. The *B*2 structure is formed from *B*1 by a contraction along one triad axis and expansion in the normal plane – a classic example of 'dilatational' transformation cited by Buerger (1951). Although no lattice translation lengths or angles are left unaltered by the transformation, it is possible to produce planes of good fit between the phases by introducing twinning or shearing, giving a martensitic texture. Fraser & Kennedy (1974) calculated the likely orientation relationships and shape changes for *B*1–*B*2 transformation products, and found them to be in accord with observation for KCl, NH_4Br and CsCl.

The study of Watanabe, Tokonami & Morimoto (1977) on the temperature-driven transformation of CsCl suggests an orientation relationship in which a {100} plane of the *B*1 phase becomes a {110} plane in the *B*2 phase and *vice versa*. These planes are also the preferred planes of contact between phases, implying that a [111] direction is not maintained constant through the transition, as would be expected for rhombohedral dilatation. The mechanism that they propose involves shear both within and between (100) layers of the *B*1 structure. Interestingly, the molecular dynamics study of Nga & Ong (1992) reproduces the mechanism of Watanabe *et al.* (1977) locally, but with a misorientation

Table 1. *Corresponding directions for the B1 and B2 structures shown in Fig. 1*

The $(010)_{B1}$ and $(110)_{B2}$ planes are in coincidence for both transformation mechanisms.

	$[uvw]_{B1}$	$[uvw]_{B2}$
(*a*)	1 0 0	1 $\bar{1}$ 2
	0 1 0	1 1 0
	0 0 1	$\bar{1}$ 1 0
(*b*)	1 0 0	1 $\bar{1}$ 1
	0 1 0	1 1 0
	0 0 1	$\bar{1}$ 1 1

between phases such that the orientation relationships expected for the dilatational mechanism are preserved overall.

A major problem with the dilatational mechanism is that the associated lattice strain has T_{2g} symmetry, whereas the only zone-centre phonons for either the *B*1 or *B*2 structure have T_{1u} symmetry. T_{1u} modes transform as $\{x,y,z\}$, and allow cation and anion sublattices to translate relative to one another. Lattice strains of T_{2g} symmetry can arise secondarily if a T_{1u} order parameter is active since T_{2g} is contained in the direct product $T_{1u}\otimes T_{1u} = A_{1g} + E_g + T_{1g} + T_{2g}$. The distinction is illustrated between geometrically feasible distortions of a structure and those which are actually consistent with lattice vibrations.

The rigid-ion lattice dynamical simulation work of Okai (1986) indicates that the TA mode in the *B*1 structure does soften with pressure, but also that there is little energetic difference between softening at the Brillouin zone centre or at the *X*-point of the zone boundary.

Transformation by softening of the TA mode is shown in Fig. 1 for (*a*) zone-centre and (*b*) zone-boundary collapse. The mechanism and orientation relationships of Watanabe *et al.* (1977) are those of Fig. 1(*b*). Those of Fig. 1(*a*) are similar to within a rotation in the plane of contact. This can be seen from Fig. 1 and Table 1. Both orientation relationships have been observed in the high-pressure neutron diffraction study of RbCl by Onodera, Kawano, Nakai & Achiwa (1992), implying that both pathways operate in that system. The Γ-point transformation proceeds *via* a polar monoclinic *Cm* intermediate, with lattice strains of T_{2g} (xz) and E_g ($x^2 - z^2$, $2y^2 - x^2 - z^2$) symmetries. The *X*-point transition state has orthorhombic symmetry (*Pnmm*; T_{2g} strain only). Okai (1986) has shown that mode softening away from the Γ-point for the *B*1 phase, and hence the orthorhombic intermediate, is favoured if the atoms are polarizable.

Yet another related transformation pathway is suggested by the observed stability of the *B*16/*B*33 structures between *B*1 and *B*2 fields for some compounds. These structures can be produced by soft-mode collapse of the *B*1 structure at 0,0,0.5 rather than 001. Such a transition state is evidently low enough in energy to become a stable intermediate TlI/GeS-like phase under pressure for compounds containing very polarizable atoms such as Pb^{2+}, Br^-, I^-, OH^- and SH^- (Chattopadhyay, von Schnering, Grosshans & Holzapfel, 1986; Haines & Christy, 1992; Adams *et al.*, 1992).

All the phases discussed above are shown in Fig. 2. All active cubic IRs correlate with T_{1u} at the zone centre. They are labelled in Fig. 2 according to the notation of Mulliken (1933) for zone-centre IRs and that of Koster, Dimmock, Wheeler & Statz (1963) for representations away from the zone centre, as used in Bradley & Cracknell (1972). Four symmetrically and thermodynamically distinct type II phase sequences are represented: *Fm3m–Cm–Pm3m*, *Fm3m–Pnmm–Pm3m*, *Fm3m–Pcmn–Bmmb* and *Bmmb–Pcmb–Pm3m*. The *Pcmn* structure is that of GeS under ambient conditions, the *Bmmb* structure that of TlI. The *Pcmb* structure appears not to have been found for a stable phase.

4.2. *The rutile, fluorite and α-PbO_2 structures*

The high-pressure transformation behaviour of rutile-structure MX_2 compounds is of interest since they may be analogues of the lower-mantle com-

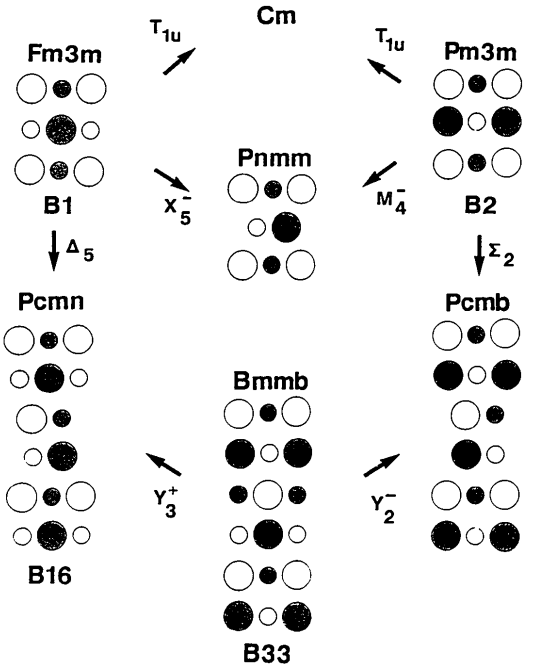

Fig. 2. Transformation paths between the *B*1–*B*2–*B*16–*B*33 structures. Viewing direction corresponds to $[101]_{B1}$ of Fig. 1, and is taken as the *y* axis for low-symmetry phases. Structure not shown for *Cm* since lattice strain is oblique to plane of paper. Shading indicates half lattice repeat height above plane of paper. The *Fm3m–Pnmm–Pm3m* path is the same as that of Fig. 1(*b*).

ponent stishovite, SiO_2. Rutile itself, TiO_2, transforms with increasing pressure to the fluorite-related monoclinic structure of baddeleyite (Sato *et al.*, 1991), which is the low-pressure structure of ZrO_2 and HfO_2. The α-PbO_2 phase appears to be stable at intermediate pressures but transformation is sluggish; this phase is more readily obtained on quenching. SnO_2 and PbO_2 transform from rutile through α-PbO_2 to the cubic fluorite structure (Ming & Manghnani, 1982); only the α-PbO_2 structure and not rutile is obtained on quenching PbO_2, whereas SnO_2 shows some inversion to the rutile structure but not to completion (Ming & Manghnani, 1982). ZnF_2 does not exhibit an α-PbO_2 phase on pressure increase, but does so on quenching (Kabalkina, Vereschagin & Lityagins, 1968). These behaviours are readily understood from consideration of the shortest rutile–fluorite transformation route.

The routes that interconnect these structures are nicely illustrated in Hyde, Bursill, O'Keeffe & Andersson (1972). Although they describe the necessary lattice distortions as 'shears', detailed consideration reveals that the lattice shear is a secondary effect in symmetric terms (as was also seen for the *B*1–*B*2 transition). The tetragonal $P4_2/mnm$ rutile structure contains a nearly hexagonal close-packed anion array in which tetragonal symmetry and a planar anion coordination environment are gained by corrugating the layers. Flattening of the layers reduces the symmetry to *Pnnm* (the $CaCl_2$ structure) and changes the anion coordination geometry to pyramidal (Fig. 3). The B_{1g} lattice mode associated with layer flattening is of systematically low frequency in rutile-structure phases (Nagel & O'Keeffe, 1971), and shows a negative pressure dependence in TiO_2 itself (Nicol & Fong, 1971).

Lability of the B_{1g} mode is crucial to the first step of the mechanism of Hyde *et al.* (1972), which assumes planar anion layers. The pseudohexagonal anion nets of the $CaCl_2$ structure are then sheared into the square nets characteristic of the fluorite structure. However, Figs. 3(*c*) and 3(*d*) show that the symmetry ascent to the fluorite structure depends not on the lattice strain but on the relative displacements of adjacent anion layers. The *Fm*3*m* symmetry of fluorite is broken by displacing alternate layers along $\pm[101]$ or equivalent. The corresponding fluorite mode belongs to the IR X_5^-, the zone boundary correlative of T_{1u} that was discussed for the *B*1/*B*2 transition. This representation is six dimensional. An orthogonal basis set for the displacement field consists of transverse anion displacement waves with $k = 100$ polarized $\parallel y$ and z, with $k = 010$ polarized $\parallel z$ and x, and with $k = 001$ polarized $\parallel x$ and y. The $CaCl_2$ structure in one of several orientations is obtained if the two components at one wavevector (say 010) are equal in magnitude and the other four components remain zero. As for the *B*1/*B*2 related phases, the xz lattice strain transforms as T_{2g}, which is contained in the reducible product $X_5^- \otimes X_5^-$ and therefore couples to the order parameter in a linear-quadratic fashion.

The $CaCl_2$ and α-PbO_2 structures share a hexagonal close-packed anion array, but the straight chains of edge-sharing octahedra in $CaCl_2$ become zigzag chains in α-PbO_2. Setting the close-packed planes $\parallel$ (010) for both structures, they can be interconverted by polysynthetic twinning on the (010) planes of $CaCl_2$, or $y/2$ slip of structural slices parallel to this plane. Thus, the structures are polytypically related, and transformation between them is usually described in terms of slip or twinning. However, the *Pnnm*, $Z' = 2$ structure of $CaCl_2$ can also be converted into the *Pcan*, $Z' = 4$ cell of α-PbO_2 as shown in Fig. 4. The intermediate *P*2/*a* and *Bmab* structures, like the *Pnnm* phase, may be obtained from fluorite in one step using the active X_5^- order parameter. However, the two equal-magnitude components that produce the $CaCl_2$ structure are unequal for the monoclinic structure, and one of them is zero for the *Bmab* structure. The energetic difference between these structures depends on the fourth-order and higher terms in the fluorite Landau expansion.

Let us write the component corresponding to y displacement modulated along the x direction as y_x, *etc.* There are five symmetrically and energetically distinct fourth-order terms in the Landau expansion,

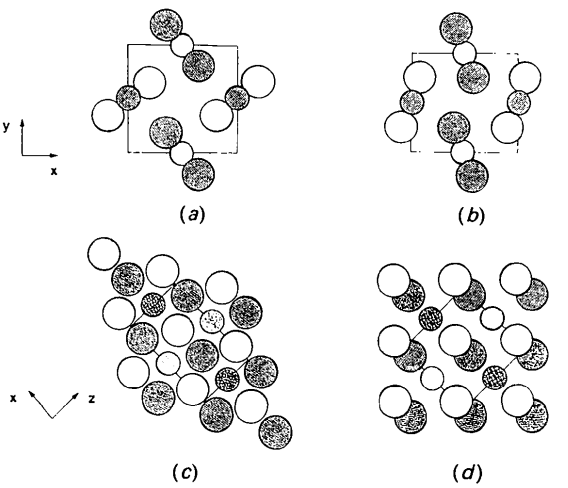

Fig. 3. (*a*) Tetragonal rutile structure viewed down the z axis. (*b*) Orthorhombic distortion of rutile structure flattens close-packed anion layers and produces $CaCl_2$ structure. (*c*) $CaCl_2$ structure viewed down the y axis. Pseudohexagonal geometry is apparent. (*d*) Lattice strain imposed on $CaCl_2$ structure so as to give a cubic unit-cell metric. Because of the displacements of successive anion layers, the symmetry remains *Pnnm*. Heights of atoms are 0 (unshaded), $\frac{1}{4}$ (light stipple), $\frac{1}{2}$ (shaded) and $\frac{3}{4}$ (heavy stipple).

which may be expressed as:

$$c_1[x_Y^4+x_Z^4+y_Z^4+y_X^4+z_X^4+z_Y^4]$$
$$c_2[x_Y^2z_Y^2+y_X^2z_X^2+x_Z^2y_Z^2]$$
$$c_3[x_Y^2x_Z^2+y_Z^2y_X^2+z_X^2z_Y^2]$$
$$c_4[x_Y^2y_X^2+y_Z^2z_Y^2+z_X^2x_Z^2]$$
$$c_5[x_Y^2z_X^2+y_Z^2x_Y^2+z_X^2y_Z^2+x_Z^2y_X^2+y_X^2z_Y^2+z_Y^2x_Z^2].$$

Depending on the values of the coefficients c_1–c_5, minimum energy is obtained with some of these terms zero and some non-zero (the c_1 term is necessarily non-zero for any deviation from the cubic fluorite structure). For each X_5^- structure of Fig. 4, the symmetry-consistent components of the IR and non-zero fourth-order terms of the Landau expansion are listed in Table 2. To facilitate comparison, one displacement is taken to be z_Y throughout. Also shown in Table 2 but not Fig. 4 is the *Pa*3 structure of pyrite, which may be stable relative to the fluorite structure for SiO_2 at extreme pressures (Park, Terakura & Matsui, 1988). The pyrite structure is derived from fluorite *via* three equal, orthogonal X_5^- displacements. It is apparent that relatively negative values of c_2 and positive c_5 favour *Pnnm* distortion of the fluorite structure, positive c_2 and negative c_5 favours *Pa*3 distortion whereas positive c_2 and c_5 favours the *Bmab* structure.

At the bottom of Fig. 4 is shown the baddeleyite structure (in a non-standard $P2_1/a$ setting), in which alternate planes of anions become symmetrically

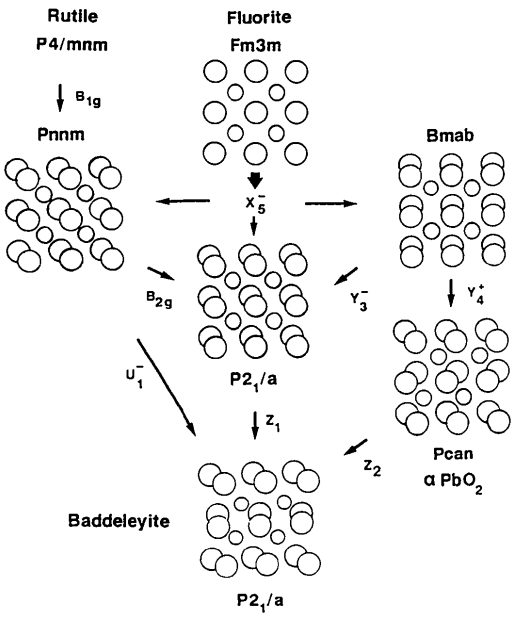

Fig. 4. Transformation paths between rutile, fluorite and α-PbO_2. The *Pnnm* structure shown is the same as that of Fig. 3(*d*). Except for this structure, the *x* axis is taken to the left, and the *z* axis vertical in the plane of the paper.

Table 2. *Active components of* X_5^- *order parameter and non-zero fourth-order Landau terms for distorted fluorites*

The equals sign indicates components constrained to be equal in magnitude.

Space group	Z'	Components	Non-zero terms
Pnnm	2	$z_Y = x_Y$	c_1 c_2
$P2_1/a$	2	z_Y x_Y y_X	c_1 c_2 c_4 c_5
Bmmb	2	z_Y	c_1
*Pa*3	4	$z_Y = y_X = x_Z$	c_1 c_5

independent. The lattice strain in the real structure reduces the anion coordination number to 7. Nevertheless, the LS relationship to the X_5^- structures is obvious. This structure clearly lies on the shortest route *between* rutile and α-PbO_2. Therefore, it is not suprising that α-PbO_2 is not readily obtained from the rutile structure of TiO_2 on increasing pressure, given the low energy of the baddeleyite structure for this compound.

Rutile and α-PbO_2 are both equally accessible from fluorite *via* the X_5^- structures. It remains to be established why the path from fluorite back to α-PbO_2 is preferred even when rutile is the stable phase. The relative signs of c_1 and c_2 may change for small distortions away from the fluorite structure. It is also possible that there are local energy maxima on the $P4_2/mnn$–*Pnnm*–*Fm*3*m* route that render it less favourable kinetically than the *Pcan*–*Bmab*–*Fm*3*m* path. To test these hypotheses, detailed calculations of internal energy as a function of structural parameters are required for the X_5^- structures.

A very different transformation behaviour that is consistent with the rutile–fluorite transformation route outlined here has recently been described for RuO_2 (Haines & Léger, 1993). This compound exhibits rutile, $CaCl_2$ and fluorite structures as stable phases, but not α-PbO_2.

The marcasite dimorph of pyrite (FeS_2) is formally the same in structure as $CaCl_2$. A transformation mechanism has been proposed for these phases that involves rotation of half of the S_2 groups (Tossell, Vaughan & Burdett, 1981; Lennie & Vaughan, 1992). The transition state is formally identical to the baddeleyite structure of Fig. 4. Transformation pathways between other structures related to marcasite, baddeleyite and so on are discussed in Christy, Haines & Clark (1992) and Haines & Léger (1993).

A recent molecular dynamics study of MgF_2 under pressure by Nga & Ong (1993) has reproduced the orientation relationship and anion motions expected for the rutile–fluorite transition as described here. They present radial density functions for an intermediate state which shows sharp Mg–Mg peaks to beyond 5 Å. The cation sublattice evidently remains intact during transformation. Distortion of the MD box shape in the intermediate state is consistent with

flattening of the close-packed anion layers (rutile–$CaCl_2$ step). Loss of maxima in the Mg–F and F–F radial density functions lead Nga & Ong to describe the intermediate state as disordered or amorphous; it may be microtwinned or of intrinsically low symmetry (baddeleyite rather than $CaCl_2$, for instance).

4.3. *The* $CaCO_3$ *phase diagram*

Calcium carbonate occurs as six known polymorphs. Vaterite (metastable) is structurally very different from the rest, and not considered further here. Calcite-I and aragonite occur more widely in nature, and are stable at relatively low and high pressure, respectively. Two high-pressure low-temperature phases (calcite-II and III) are known, which are formed readily from calcite-I. The transitions from calcite-I to II and III lie within the aragonite stability field, so phases II and III appear to be metastable. A recent study by Hess, Ghose & Exarhos (1991) shows them in a topologically consistent pressure–temperature diagram as 'stable in the laboratory timeframe', but the calcite-I–aragonite transition is placed at a much higher pressure than is usual (*ca* 14 kbar at < 473 K).

At high temperature (> 1263 K), rotational disordering of the calcite CO_3 ions occurs (Dove & Powell, 1989). In addition to the soft Z-point mode giving the high-temperature phase, there is a soft F-point mode implying incipient ordering on a different scheme. The high-temperature F-points become F and L symmetry points in calcite-I. Anomalous inelastic neutron scattering has been observed at the calcite-I L-points, which has been interpreted as dynamic fluctuation between ordering schemes (Dove *et al.*, 1992). The associated entropy causes curvature in the calcite–aragonite equilibrium boundary, which has been modelled by Redfern, Navrotsky & Salje (1989).

Calcite-I, calcite-II and aragonite all share (pseudo)hexagonal planes of carbonate ions as a structural element. In calcite-I, these are parallel to (0001); in aragonite, they are on (001). The structure of calcite-II was determined by Merrill & Bassett (1975), who found it to be a simple modification of that of calcite-I. In calcite-I, the CO_3 groups are oriented so as to have C—O bonds pointing down the **x** axes of the structure. In calcite-II, adjacent CO_3 groups are counter-rotated by 11°. Continued rotation to 30° from their initial orientation produces the carbonate layer of the aragonite structure (Fig. 5). The topotactic relationships observed by Gillet, Gérard & Williame (1987) are consistent with the carbonate layers being preserved during calcite–aragonite transformation. Those observed by McTigue & Wenk (1985) imply disruption of the layers, but were observed in a thin electron microscope specimen and may correspond to a surficial transformation mechanism.

The displacements associated with the calcite-I–II transition are consistent with a soft F_2^- mode in calcite-I, inherited from the high-temperature F-point instability. In the classification of this paper, the transition is type I, whether first or second order thermodynamically. The Landau theory of the transformation has been discussed by Hatch & Merrill (1981), who showed that the transformation is allowed to be second order by symmetry. Hess *et al.* (1991) obtained a soft F_2^- mode in a lattice dynamics simulation of calcite; their Raman study showed that the transformation is thermodynamically first order at room temperature. Below, it is shown that calcite-II is an intermediate on the shortest calcite–aragonite path.

Table 3 compares lattice parameters for a pseudo-monoclinic $C2/c$ calcite-I cell ($x_{mon} = [120]_{hex}$, $z_{mon} = [121]_{hex}$), calcite-II at 1.5 GPa in the corresponding $P2_1/n$ setting, and aragonite. The carbonate-ion planes are parallel to (001) in each case. It can be seen that the lattice strains involved in the calcite-II transformation are very small, and those between calcite-II and aragonite only a few percent.

Fig. 6 shows the full calcite-I–calcite-II–aragonite transformation pathway. Calcite-I is shown in the metrically monoclinic cell of Table 3. The $P2_1/n$

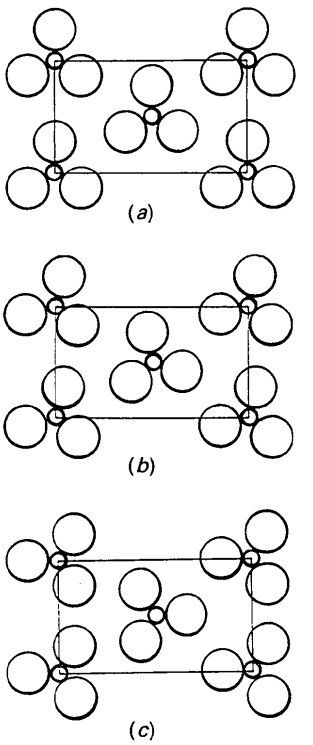

Fig. 5. (*a*) The CO_3 layer of calcite. (*b*) The CO_3 layer of calcite-II at 15 kbar. (*c*) The idealized CO_3 layer of aragonite.

Table 3. *Comparison of corresponding cell parameters for* $CaCO_3$ *phases*

Cell parameters were calculated from Merrill & Bassett (1975) and Wyckoff (1964). Monoclinic cell used for calcite to facilitate direct comparison with other phases.

Phase	Space group	a (Å)	b (Å)	c (Å)	β (°)
Calcite-I	$C2/c$ ($R\bar{3}c$)	8.64	4.99	6.38	116.9
Calcite-II	$P2_1/n$	8.71	4.98	6.63	118.6
Aragonite	$Pcmn$	7.97	4.96	5.74	90.0

structure shown is more distorted than the refined structure of calcite-II: the carbonate groups have been rotated by a full 30° so as to be like those of aragonite in orientation, and alternate carbonate layers have been translated by $\pm b/4$. The cell parameters shown are also intermediate between those of the calcite phases and those of aragonite. Nevertheless, this structure is still formally that of calcite-II. Examination of the relationship between calcite-I, calcite-II and aragonite structures reveals that the other principal change required to produce aragonite from calcite is slip of the cation and anion sublattices relative to one another. This requires an acentric intermediate ($P2_1$) between the $P2_1/n$ structure and the $P2_1/m$ structure shown in Fig. 5 (these three structures constitute another type II HS1–LS–HS2 triplet).

Although Fig. 5 shows that a relatively short (four step) transformation path exists between calcite-I and aragonite, these phases are known to transform at high temperature by grain-boundary nucleation in polycrystalline material (Hacker, Kirby & Bowles, 1992). This implies that there are energetically prohibitive barriers to be overcome on the short paths. The existence of calcite-II at high pressure and low temperature pinpoints the unfavourable step as the polar phase between calcite-II and aragonite. Calcite-II is understood to be an intermediate on the shortest calcite-I/aragonite transformation route that is observed because the next stage is kinetically inaccessible.

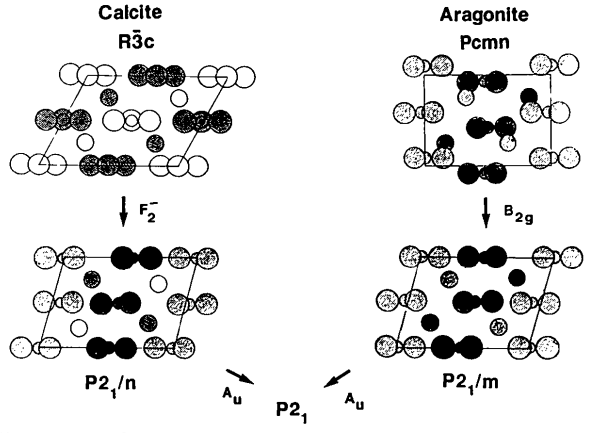

Fig. 6. Transformation path from calcite to aragonite. Heights indicated by shading as for Fig. 2. Note corrugation of the carbonate layers in the real aragonite structure, which avoids close O—O contacts.

5. Concluding remarks

Many phase transitions show a mixture of 'reconstructive', 'displacive' and 'order–disorder' features. Therefore, these terms are not always useful for classifying transformations. Analysis of the symmetry changes involved in them allows rigorous classification into three types: (I) HS–LS, (II) HS1–(LS transition state)–HS2 or converse, (III) cascades of such elementary steps. The shortest possible type III routes between known structures are often found to be only three or four steps long. At the other extreme, descent into a fully amorphous intermediate state is still type III. It is likely that short type III transformation paths are important in at least the nucleation stage of many transformations. The appropriate transition states may have been observed experimentally in PbO. Analysis of the shortest pathways is shown to provide insight into the behaviour of several systems.

Although a molecular dynamics simulation of the $B1$–$B2$ transition predicts the two shortest possible routes as transformation mechanisms, the stability of $B16/B33$ intermediate structures suggests that a longer pathway operates when a very polarizable species is present. The quenching of high-pressure fluorites into the α-PbO_2 structure rather than rutile is seen as a consequence of the high degeneracy of the fluorite lattice mode involved on the shortest fluorite–rutile path, and the difficulty of nucleating the α-PbO_2 phase of TiO_2 on pressure increase as a result of the thermodynamic stability of the baddeleyite intermediate at even higher pressure. Calcite-II is seen to be a kinetically blocked intermediate phase on the shortest calcite–aragonite route.

Analysis of the shortest multistage transformation routes as described here is a straightforward *a priori* investigation of symmetric relationships between phases and their possible transformation behaviour. Predictions may be tested against experimental observations using molecular dynamics simulation.

I am indebted to Dr Julian Haines for discussions which have much improved this paper.

References

ADAMS, D. M., CHRISTY, A. G., HAINES, J. & CLARK, S. M. (1992). *Phys. Rev. B*, **46**, 11358–11367.
BIRMAN, J. L. (1966). *Phys. Rev. Lett.* **17**, 1216–1219.
BOYLE, L. L., WALKER, J. R. & WANJIE, A. C. (1980). *Faraday Discuss.* **69**, 115–119.

BRADLEY, C. J. & CRACKNELL, A. P. (1972). *The Mathematical Theory of Symmetry in Solids*. Oxford Univ. Press.
BUERGER, J. M. (1951). In *Phase Transformation in Solids*, edited by R. SMOLUCHOWSKI, J. E. MAYER & W. A. WEYL. New York: Wiley.
CHATTOPADHYAY, T., VON SCHNERING, H. G., GROSSHANS, W. A. & HOLZAPFEL, W. B. (1986). *Physica B/C*, **139/140**, 356–360.
CHRISTY, A. G., HAINES, J. & CLARK, S. M. (1992). *J. Phys. Condens. Matter*, **4**, 8131–8140.
DELAEY, L. (1991). *Diffusionless Transformations*. In *Phase Transformations in Materials, Material Science and Technology* 5, edited by P. HAASEN. New York: VCH Publishers.
DMITRIEV, V. P., GUFAN, YU. M. & TOLÉDANO, P. (1991). *Phys. Rev. B*, **44**, 7248–7255.
DMITRIEV, V. P., ROCHAL, S. B., GUFAN, YU. M. & TOLÉDANO, P. (1988). *Phys. Rev. Lett.* **60**, 1958–1961.
DMITRIEV, V. P., ROCHAL, S. B., GUFAN, YU. M. & TOLÉDANO, P. (1989). *Phys. Rev. Lett.* **62**, 2495–2498.
DORNBERGER-SCHIFF, K. (1959). *Acta Cryst.* **9**, 593–601.
DOVE, M. T., HAGEN, M. E., HARRIS, M. J., POWELL, B. M., STEIGENBERGER, U. & WINKLER, B. (1992). *J. Phys. Condens. Matter*, **4**, 2761–2774.
DOVE, M. T. & POWELL, B. M. (1989). *Phys. Chem. Miner.* **16**, 503–507.
DUROVIC, S. & WEISS, Z. (1986). *Bull. Soc. Fr. Minéral.* **109**, 15–29.
ERNST, G., ARTNER, C., BLASCHKO, O. & KREXNER, G. (1986). *Phys. Rev. B*, **33**, 6465–6469.
FRASER, W. L. & KENNEDY, S. W. (1974). *Acta. Cryst.* A**30**, 13–22.
GILLET, PH., GÉRARD, Y. & WILLIAME, C. (1987). *Bull Soc. Fr. Minéral.* **110**, 481–496.
HACKER, B. R., KIRBY, S. H. & BOWLES, S. R. (1992). *Science*, **258**, 110–113.
HAINES, J. & CHRISTY, A. G. (1992). *Phys. Rev. B*, **46**, 8797–8805.
HAINES, J. & LÉGER, J. M. (1993). *Phys. Rev. B*. In the press.
HATCH, D. M. & MERRILL, L. (1981). *Phys. Rev. B*, **23**, 368–374.
HESS, N. J., GHOSE, S. & EXARHOS, G. (1991). In *Recent Trends in High-Pressure Research* (*Proc* XIII *AIRAPT Conference*), edited by A. K. SINGH. New Delhi, Bombay, Calcutta: Oxford and IBH Publishing.
HYDE, B. G., BURSILL, L. A., O'KEEFFE, M. & ANDERSSON, S. (1972). *Nature* (*London*) *Phys. Sci.* **237**, 35–38.
KABALKINA, S. S., VERESCHAGIN, L. F. & LITYAGINS, L. M. (1968). *Sov. Phys. Dokl.* **12**, 946–949.
KOSTER, G. F., DIMMOCK, J. O., WHEELER, R. G. & STATZ, H. (1963). *Properties of the Thirty-Two Point Groups*. Cambridge: MIT Press.
LANDAU, L. D. & LIFSHITZ, E. M. (1958). *Statistical Physics*. Reading: Addison-Wesley.
LENNIE, A. R. & VAUGHAN, D. J. (1992). *Am. Mineral.* **77**, 1166–1171.
MCTIGUE, J. W. & WENK, H.-R. (1985). *Am. Mineral.* **70**, 1253–1261.
MERRILL, L. & BASSETT, W. A. (1975). *Acta Cryst.* B**31**, 343–348.
MING, L. C. & MANGHNANI, M. H. (1982). In *High-Pressure Research in Geophysics*, edited by S. AKIMOTO & M. H. MANGHNANI. Tokyo: Centre Academic.
MULLIKEN, R. S. (1933). *Phys. Rev.* **43**, 279–302.
NAGEL, L. & O'KEEFFE, M. (1971). *Mater. Res. Bull.* **6**, 1317–1320.
NGA, Y. A. & ONG, C. K. (1992). *Phys. Rev. B*, **46**, 10547–10553.
NGA, Y. A. & ONG, C. K. (1993). *J. Chem. Phys.* **98**, 3240–3245.
NICOL, M. & FONG, M. Y. (1971). *J. Chem. Phys.* **54**, 3167–3170.
OKAI, B. (1986). *Physica B/C*, **139/140**, 221–223.
ONODERA, A., KAWANO, S., NAKAI, Y. & ACHIWA, N. (1992). *Physica, B*, **180/181**, 279–280.
PARK, K. T., TERAKURA, K. & MATSUI, Y. (1988). *Nature* (*London*), **336**, 670–672.
PUTNIS, A. & MCCONNELL, J. D. C. (1979). *Principles of Mineral Behaviour*. Cambridge Univ. Press.
REDFERN, S. A. T., NAVROTSKY, A. & SALJE, E. K. H. (1989). *Contrib. Mineral. Petrol.* **101**, 479–484.
SALJE, E. K. H. (1991). *Acta Cryst.* A**47**, 453–469.
SATO, H., ENDO, S., SUGIYAMA, M., KIKEGAWA, T., SHIMOMURA, O. & KUSABA, K. (1991). *Science*, **251**, 786–788.
SCHOONOVER, R., GROY, T. L. & LIN, S. H. (1989). *J. Solid State Chem.* **83**, 207–213.
SHOJI, H. (1931). *Z. Kristallogr.* **77**, 381–410.
TOSSELL, J. A., VAUGHAN, D. J. & BURDETT, J. K. (1981). *Phys. Chem. Miner.* **7**, 177–184.
WATANABE, M., TOKONAMI, M. & MORIMOTO, N. (1977). *Acta Cryst.* A**33**, 294–298.
WYCKOFF, R. W. G. (1964). *Crystal Structures*. New York: Interscience.

Acta Cryst. (1993). B**49**, 996–1001

Determination of Crystal Structures from Limited Powder Data Sets: Crystal Structure of Zirconium Phenylphosphonate

BY M. D. POOJARY, H.-L. HU, F. L. CAMPBELL III AND A. CLEARFIELD

Department of Chemistry, Texas A&M University, College Station, Texas 77843, *USA*

(*Received* 27 *October* 1992; *accepted* 2 *July* 1993)

Abstract

The structure of zirconium phenylphosphonate, $Zr(O_3PC_6H_5)_2$, was solved based on a combination of modeling techniques and Patterson methods and refined by Rietveld methods. Powder diffraction data were collected using synchrotron radiation (λ = 1.3087 Å). The crystals belong to the space group $C2/c$ with $a = 9.0985\ (5)$, $b = 5.4154\ (3)$, $c = 30.235\ (2)$ Å and $\beta = 101.333\ (5)°$. The reliability factors are $R_{wp} = 0.129$, $R_p = 0.095$, $R_F = 0.023$ and the statistically expected $R_{wp} = 0.02$. In the c-axis projection the structure resembles very closely that of α-zirconium phosphate. The phenyl groups are inclined by about 30° to the c axis and also tilted from the ab plane. The C-center-related phenyl